

Supplementary Discussion

Sequence and cell-type determinants of RNA base edits induced by BE3 and ABEmax

The base edits we observed preferentially occur within specific short sequence motifs (ACW for Cs and UA for As) although we do not yet understand why some bases embedded in these motifs are edited while others are not. Attempts to identify other, more extended motifs using the WebLogo tool³⁶ did not reveal any obvious strongly conserved sequences within 100 bps upstream or downstream of the ACW or UA motifs (**Extended Data Figs. 9a-9d**). Despite some commonality in the positions of edited C bases identified in our HepG2 and HEK293T cell experiments with BE3, we expect that the range and frequencies of edits for both cytosine and adenine base editors will likely vary among cell types, at least in part due to differences in transcript expression profiles. Although cellular co-factors previously reported to modify APOBEC1 function might also modulate cell-type-specific activity of BE3 and other rAPOBEC1-containing CBEs³⁷⁻³⁹, a recent report suggests that one of these factors (A1CF) may not even be required for RNA editing^{38,40}.

Predicting potential impacts of off-target RNA editing using in silico methods

As noted in the main text, the widespread nature of RNA edits induced by base editors makes it challenging to design and conduct experiments that can assess the functional consequences of these alterations in human cells. Here we provide the results of three *in silico* analyses aimed at illustrating some potential impacts of the RNA edits we observed with BE3 and ABEmax and how the SECURE variants can reduce these effects for BE3. However, it is important to note that each of these approaches has limitations and caveats (described in each section below) and that no causality for a functional consequence should be inferred from these findings. In addition, we wish to emphasize that these purely bioinformatic-based approaches do not serve as a substitute for careful experimental analyses.

(1) **RNA edits within tumor suppressor genes (TSGs).** For this analysis, we assessed whether C-to-U (induced by BE3) or A-to-I (induced by ABEmax) RNA edits would be predicted to create missense, nonsense (for BE3 only because ABEs cannot do so), and splice region mutations in expressed TSGs (**Supplementary Methods**). Results of these analyses are presented in **Supplementary Table 35 (Tab1)**. For BE3, we detected predicted missense and nonsense (but no splice region) mutations that might potentially alter function in multiple TSGs in both HepG2 and HEK293T cells. Interestingly, certain TSGs (e.g., *MSH2* and *MSH6*) harbored higher numbers of predicted mutations. As expected, the number of mutations per gene and the number of TSGs mutated generally increased with higher expression levels of BE3 in HEK293T cells (comparing all GFP+ with the top 5% GFP sorted cells). Importantly, the SECURE BE3 variants showed dramatically different results with BE3-R33A predicted to induce only a single edit in one TSG (a predicted nonsense mutation in *MAP2K4*) and with BE3-R33A/K34A not predicted to induce any mutations in any TSG. ABEmax also induced predicted missense mutations (but no splice region mutations) in multiple TSGs expressed in HEK293T cells. Although these RNA edits lie within expressed TSGs, we do not know which, if any, of these alterations would actually lead to loss or alteration of function, something that can only be ascertained experimentally.

(2) **RNA edits in microRNA (miRNA) binding sites.** We examined whether BE3- or ABEmax-mediated RNA edits that were induced in any of 182,487 3' UTR miRNA binding sites previously validated in a range of different human cells (**Supplementary Methods**). The results of this analysis are shown in **Supplementary Table 35 (Tab2)**. In experiments with the top 5% GFP-positive cells using wild-type BE3 and the *RNF2* gRNA, we found that edits induced in HEK293T and HepG2 cells lie within 12,870 and 9,884 validated miRNA binding sites, respectively. Notably, in parallel experiments with the BE3-R33A variant and the *RNF2* gRNA, we found edits induced in HEK293T and HepG2 cells occur within sequences of 83 and 14 validated miRNA binding sites, respectively. With the BE3-R33A/K34A and the *RNF2* gRNA, no edits induced in either cell line fell within any validated miRNA binding sites. With ABEmax and the

HEK site 2 gRNA, we found edits induced in HEK293T cells occur within 1,079 validated miRNA binding sites. However, an important caveat to note for all of these results is that we do not know which, if any, of these RNA edits actually negatively impact miRNA binding to these sites.

(3) **RNA edits predicted to generate potential neoantigens.** We used a bioinformatic approach to predict whether missense mutations induced by BE3 or ABEmax might be expected to create potential neoantigens (**Supplementary Methods**). These findings are summarized in **Supplementary Table 35 (Tab3)**. In experiments with the top 5% GFP-positive cells using BE3 and the *RNF2* gRNA, our analysis identified 8,875 and 3,443 predicted potential neoantigens in HEK293T and HepG2 cells, respectively; these numbers were reduced to 52 and 11 predicted potential neoantigens with BE3-R33A and 1 and 1 predicted potential neoantigens with BE3-R33A/K34A. ABEmax expressed with HEK site 2 gRNA in the top 5% of GFP-positive HEK293T cells yielded 3,140 predicted potential neoantigens. It is important to emphasize the following caveats for these analyses: (1) these numbers represent only predictions and the only way to actually prove neoantigen creation will be through experiments and (2) it is not clear whether these predicted neoantigens would actually be expressed or have any functional consequences in HEK293T or HepG2 cells.

Assessing impacts of off-target RNA editing on cell viability

We transfected HEK293T cells in triplicate with plasmids expressing the *RNF2* gRNA and either nCas9-UGI-NLS, wild-type BE3, BE3-R33A, BE3-R33A/K34A, and BE3-E63Q (each as 2A fusions to GFP). GFP-positive cells were sorted 36 hours post-transfection (all GFP-sorting, see **Methods**) and then equal numbers of viable sorted cells (as determined by acridine orange/propidium iodide staining) were plated into three technical replicate wells per biological replicate for four timepoints (**Supplementary Methods**). At various timepoints post-plating (days 1, 2, 3, and 4), we performed a cell viability assay (CellTiter-Glo) for each biological replicate (n=3) in technical triplicates (**Supplementary Methods**). In

this assay, mean luminescence RLU values are an indirect measure of ATP content, which is directly proportional to the number of viable cells. The results of these experiments (**Extended Data Fig. 9e** and **Supplementary Tables 36**) show a modest decrease in mean cell viability for wild-type BE3 relative to that of the nCas9 control at all four days (ranging from 68% to 80% RLU relative to nCas9-UGI-NLS, $p < 0.001$ for days 2, 3 and 4 – significant after multiple testing correction; **Supplementary Table 36**). By contrast, the mean cell viabilities of the BE3-R33A/K34A and the BE3-E63Q (catalytically inactive) variants are similar to or higher than that of the nCas9-UGI-NLS control (minimum RLU of 95% relative to nCas9-UGI, no significant decreases; **Extended Data Fig. 9e** and **Supplementary Table 36**). The BE3-R33A variant mean relative RLU value initially resembles that of wild-type BE3 (reduction to 76%) but then begins to resemble that of nCas9 by days 3 and 4 (reductions to 90% and 90%, nominally significant with $p < 0.05$). (Additional details of the statistical test are described in **Supplementary Methods**.) In sum, this experiment shows that wild-type BE3 induces a modest but statistically significant negative effect on cell viability when compared to nCas9-UGI-NLS whereas the two SECURE-BE3 variants show either a smaller negative effect (BE3-R33A) or no detectable effect (BE-R33A/K34A).

We note that there are several reasons why this experimental setup might detect only a modest effect of wild-type BE3 on cell viability: First, the negative impacts of transfection and FACS procedures on cell health are likely more substantial than that of the base editor. The effects of these experimental procedures are controlled for with the nCas9-UGI and the BE3-E63Q negative controls but it is likely that a large proportion of the dynamic range of the cell viability assay is lost due to the early toxicity induced by those two procedures. Second, because we are performing transient transfection, there will be a great deal of heterogeneity in the numbers, frequencies, and combinations of RNA edits induced in any given cell in the population. Hence, it may be challenging to observe any toxic effects due to this heterogeneity and an inducible, stable expression system will likely be better suited to detect cell

viability effects. Finally, it is also possible that both pro- and anti-proliferative edits may exist in the same or different cells and this might therefore offset any anti-proliferative effects as well.

Supplementary Methods

Prediction of tumor suppressor gene mutations by RNA editing

RNA off-target edits occurring in all three replicates (or for SECURE variants, edits occurring in any of the three replicates) were filtered to include only those resulting in missense, nonsense and splice region mutations, as classified by VEP (see **RNA sequence variant effect prediction** section in **Methods**). A list of 82 tumor suppressor genes (TSGs) was downloaded from GSEA MSigDB (MSigDB database version 6.2; GSEA/MSigDB website version 6.3⁴¹). Only TSGs expressed in a cell-type specific manner in our dataset were considered.

Prediction of miRNA binding site disruption by RNA editing

All RNA off-target edits occurring in all three replicates (for SECURE variants, edits occurring in any of the three replicates) were considered. Experimentally validated human miRNA target regions were downloaded from Ensembl Regulation version 92 for the GRCh38.p12 reference genome, and filtered to those in 3'UTRs, using Ensembl version 92 annotations.

Neoantigen prediction

RNA off-target edits occurring in all three replicates (for SECURE variants, edits occurring in any of the three replicates) were filtered to include only those resulting in missense variants, as classified by VEP (see **RNA sequence variant effect prediction** section in **Methods**). Reference protein sequences corresponding to these variants were then retrieved using biomaRt⁴² on Ensembl version 92 annotations and substituted with the corresponding mutated amino acids in their respective positions. Recoded protein sequences were then digested into 8,9,10,11,12,13 and 14-mer long peptides. Peptide k-mers

that were different from their reference counterparts were then input into netMHC⁴³ version 4.0 for HLA supertypes (HLA-A0101, HLA-A0201, HLA-A0301, HLA-A2402, HLA-A2601, HLA-B0702, HLA-B0801, HLA-B2705, HLA-B3901, HLA-B4001, HLA-B5801, HLA-B1501) with a threshold for strong binding of 0.1.

Cell viability assay

HEK293T (2.5×10^6 cells) cells were seeded into 100mm TC-treated culture dishes (Fisher) 24h prior to transfection. Cells were transfected in triplicate with 16.5 μ g of BE3, BE3(E63Q), SECURE-BE3 or negative control plasmids as well as 5.5 μ g of guide RNA expression plasmid (*RNF2* site1), and 66 μ L TransIT-293T. Cells were incubated for 36h post-transfection, followed by sorting for GFP-positive cells (as described in **FACS Methods**). After sorting, cells were counted using a LUNA-FL Cell Counter (Logos Biosystems) with Acridine Orange/Propidium Iodide Stain. 5×10^3 viable cells were seeded into 96-well solid white TC-treated microplates (Corning) in 100 μ L DMEM; each condition was seeded into 3 wells for technical triplicates per biological replicate (n=3 biologically independent samples), and 4 plates of cells were prepared from this experiment for 4 different endpoints (d1-d4). At 24h, 48h, 72h, and 96h post-sorting, cell viability was determined using the CellTiter-Glo Luminescent Cell Viability Assay reagent (Promega). After the plate was equilibrated at room temperature for 30 minutes, 100 μ L of 1:5 diluted CellTiter-Glo reagent were directly added to each well (adapted from ref. 44). After 2 minutes of plate shaking on the Synergy HT microplate reader (BioTek), plates were incubated at room temperature for 10 minutes, and read with the Synergy HT for luminescence. The luminescence background (average of 8 empty wells per plate) was subtracted from all luminescence values generated in the respective plate. Cells were not seeded at the edge of the plate (columns 1 and 12 as well as rows A and H).

Statistical testing for differences in the cell viability assay data

We fit a linear mixed effects model using the R nlme package with log₂ (RLU) as the outcome to assess the effect on cell viability of each base editor variant compared to nCas9-UGI-NLS. A random effect for

biological replicate was used to account for the correlation between technical replicates. P-values represent the significance of the fixed effect coefficient encoding the base editor in the mixed-effects models.

References for Supplementary Discussion and Supplementary Methods

- 37 Mehta, A., Kinter, M. T., Sherman, N. E. & Driscoll, D. M. Molecular cloning of apobec-1 complementation factor, a novel RNA-binding protein involved in the editing of apolipoprotein B mRNA. *Mol Cell Biol* **20**, 1846-1854 (2000).
- 38 Fossat, N. *et al.* C to U RNA editing mediated by APOBEC1 requires RNA-binding protein RBM47. *EMBO Rep* **15**, 903-910, doi:10.15252/embr.201438450 (2014).
- 39 Yamanaka, S., Poksay, K. S., Driscoll, D. M. & Innerarity, T. L. Hyperediting of multiple cytidines of apolipoprotein B mRNA by APOBEC-1 requires auxiliary protein(s) but not a mooring sequence motif. *J Biol Chem* **271**, 11506-11510 (1996).
- 40 Snyder, E. M. *et al.* APOBEC1 complementation factor (A1CF) is dispensable for C-to-U RNA editing in vivo. *RNA* **23**, 457-465, doi:10.1261/rna.058818.116 (2017).
- 41 Subramanian, A. *et al.* Gene set enrichment analysis: a knowledge-based approach for interpreting genome-wide expression profiles. *Proc Natl Acad Sci U S A* **102**, 15545-15550, doi:10.1073/pnas.0506580102 (2005).
- 42 Kinsella, R. J. *et al.* Ensembl BioMart: a hub for data retrieval across taxonomic space. *Database (Oxford)* **2011**, bar030, doi:10.1093/database/bar030 (2011).
- 43 Andreatta, M. & Nielsen, M. Gapped sequence alignment using artificial neural networks: application to the MHC class I system. *Bioinformatics* **32**, 511-517, doi:10.1093/bioinformatics/btv639 (2016).
- 44 Joung, J. *et al.* Genome-scale CRISPR-Cas9 knockout and transcriptional activation screening. *Nat Protoc* **12**, 828-863, doi:10.1038/nprot.2017.016 (2017).

Supplementary Note

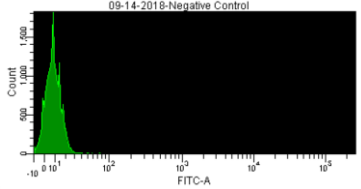
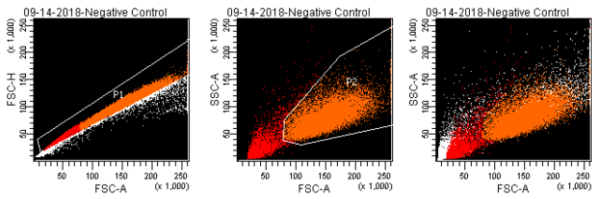
FACS raw data and gating examples for different experimental conditions.

The following figures describe how control and base editor expressing cells were sorted. We show examples of HEK293T and HepG2 cell sorting strategies under different experimental conditions. The image data was generated at the MGH Molecular Pathology Flow Cytometry Core Facility on a BD FACSAria II cytometer using BD FACSDiva v. 6.1.3. The data shown is taken from original batch analysis files. We exclusively sorted GFP+ cells. The dot and contour plots shown were used to exclude doublets, gate for the cell population and sort for GFP+ cells. The x-axis shows FITC as the fluorochrome used, closely matching the spectral characteristics of GFP.

BD FACSDiva 6.1.3
Batch Analysis

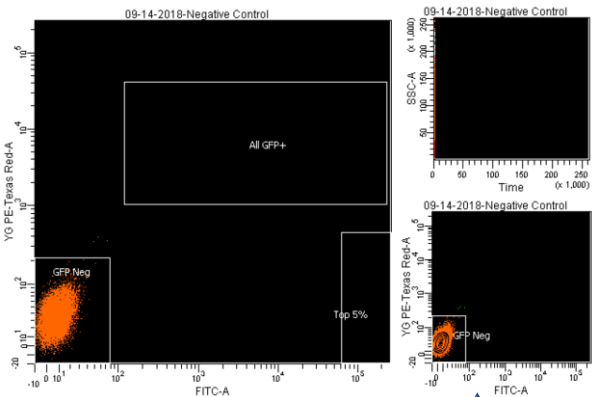
FACS Raw Data Analysis Legends

Doublet exclusion



Population histogram

Gating for GFP+ cells



Tube: Negative Control			
Population	#Events	%Parent	%Total
All Events	30,000	###	100.0
P1	21,968	73.2	73.2
P2	18,616	84.7	62.1
Top 5%	0	0.0	0.0
GFP Neg	18,613	100.0	62.0
All GFP+	0	0.0	0.0

Population statistics

Experiment Name: EJUL				
Specimen Name: 09-14-2018				
Tube Name: Negative Control				
Record Date: Sep 14, 2018 10:33:33 AM				
\$OP: JoungLab				
GUID: e73e0bba-2fcf-4511-aab0-a4907b335921				
Population	#Events	%Parent	FITC-AYG PE-Texa... Mean	Mean
Top 5%	0	0.0	###	###
GFP Neg	18,613	100.0	8	36
All GFP+	0	0.0	###	###

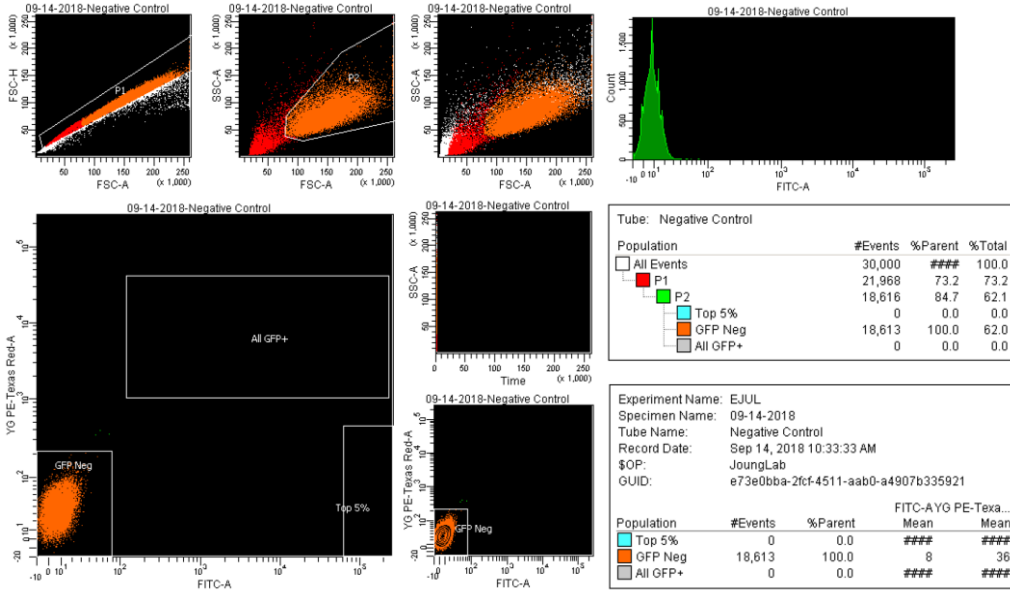
Experiment details/date

Population statistics

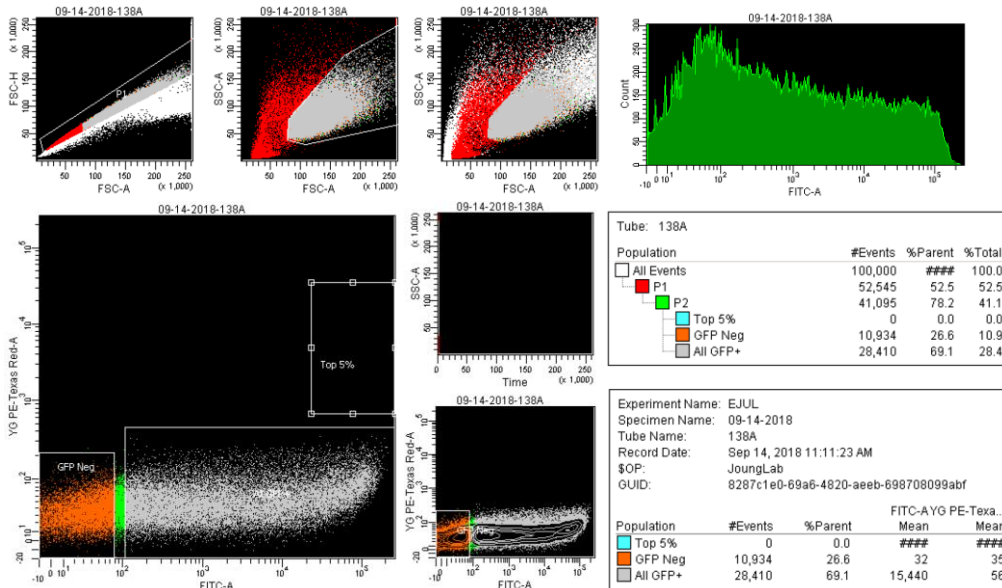
Contour plot

HEK293T cells

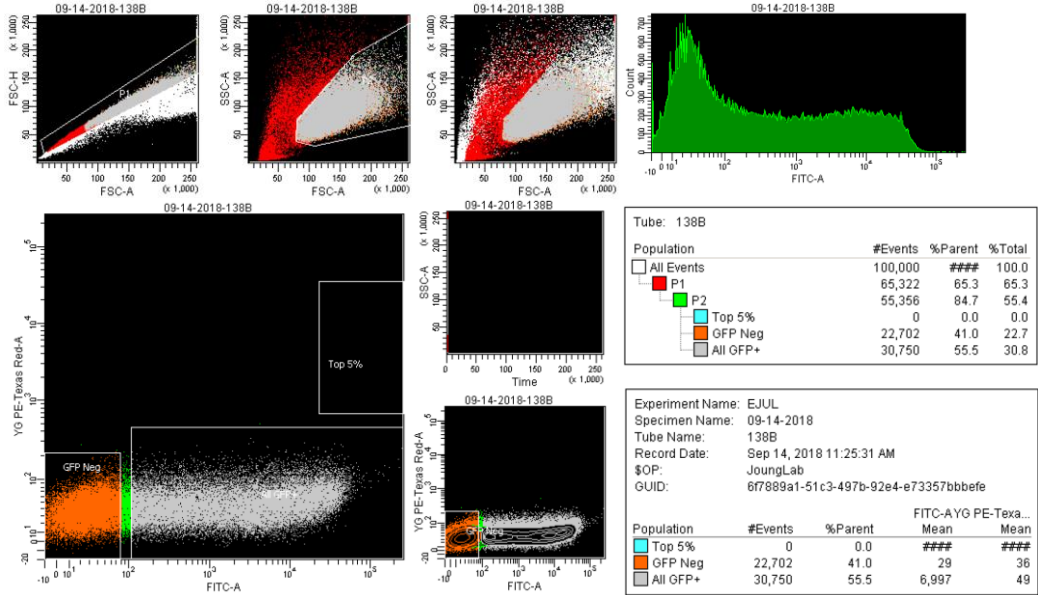
HEK293T Negative Control (no transfection)



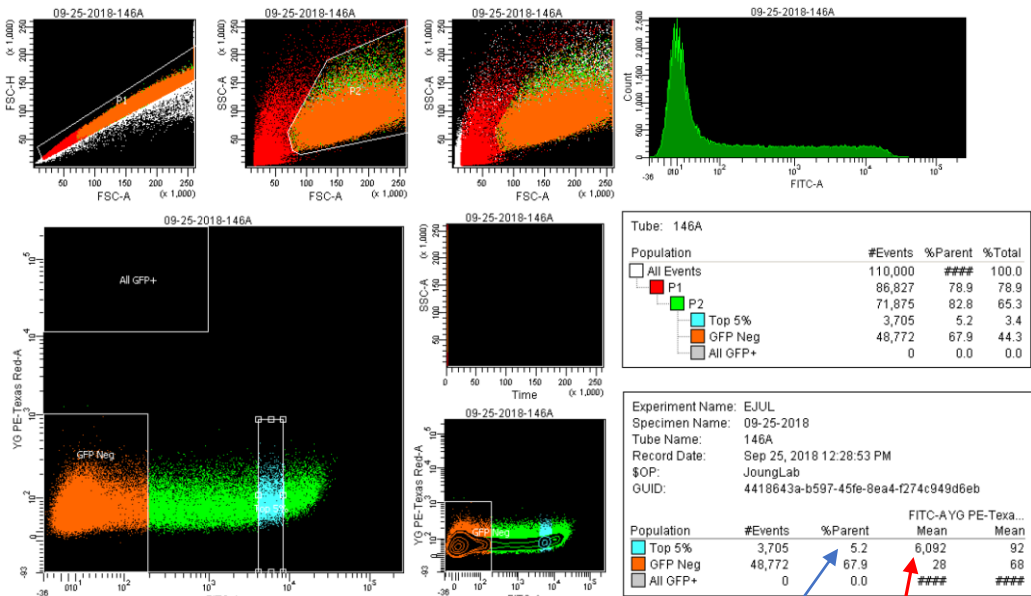
HEK293T **All GFP+** nCas9-UGI-NLS Control



HEK293T All GFP+ BE3-treated

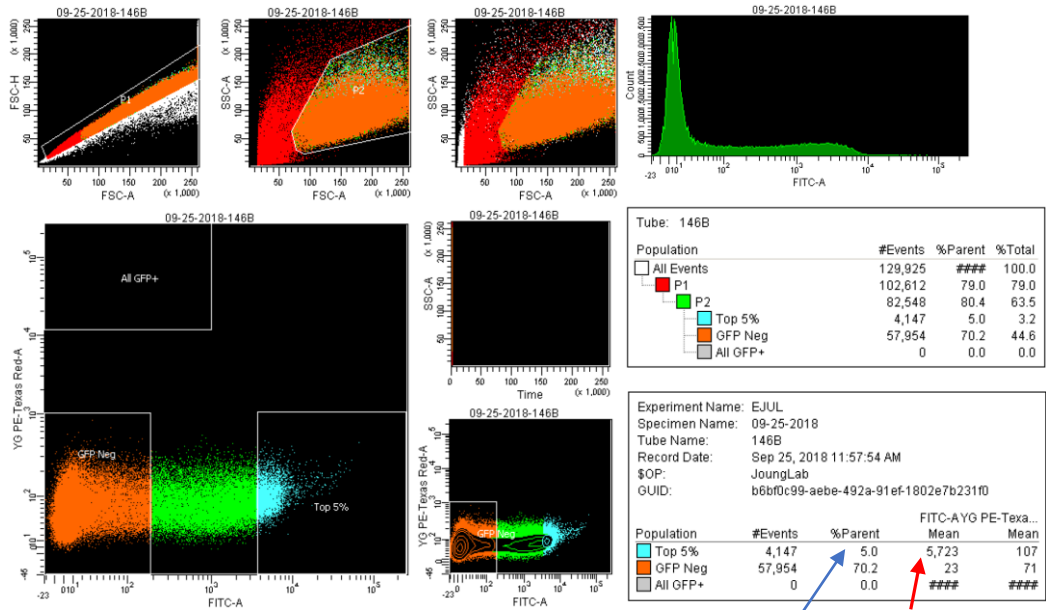


HEK293T Top 5%-matched nCas9-UGI-NLS Control for BE3



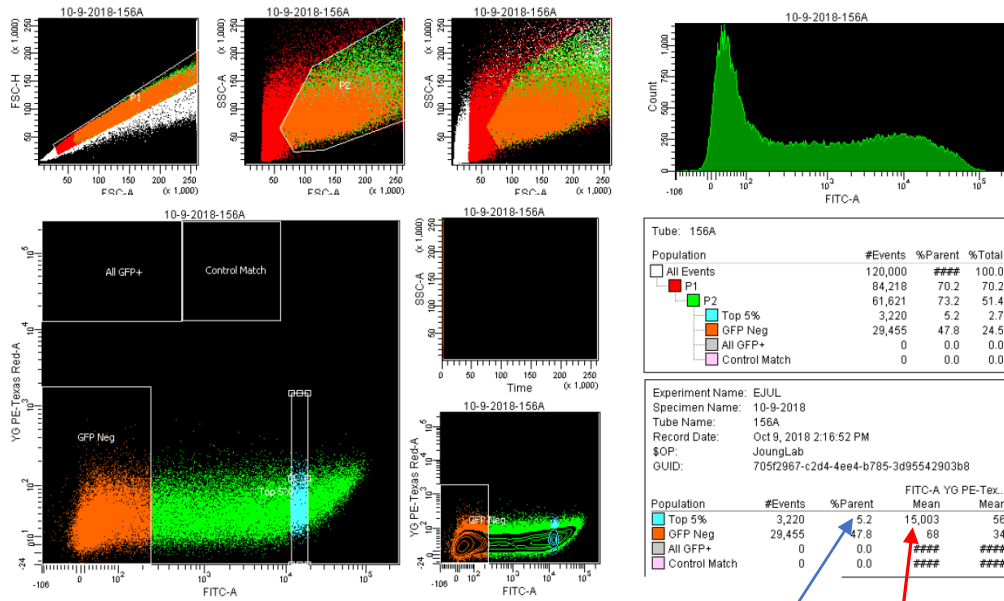
5% population with **GeoMean (MFI)**
 matched to top 5% BE-treated cells (see next slide)

HEK293T Top 5% BE3-treated



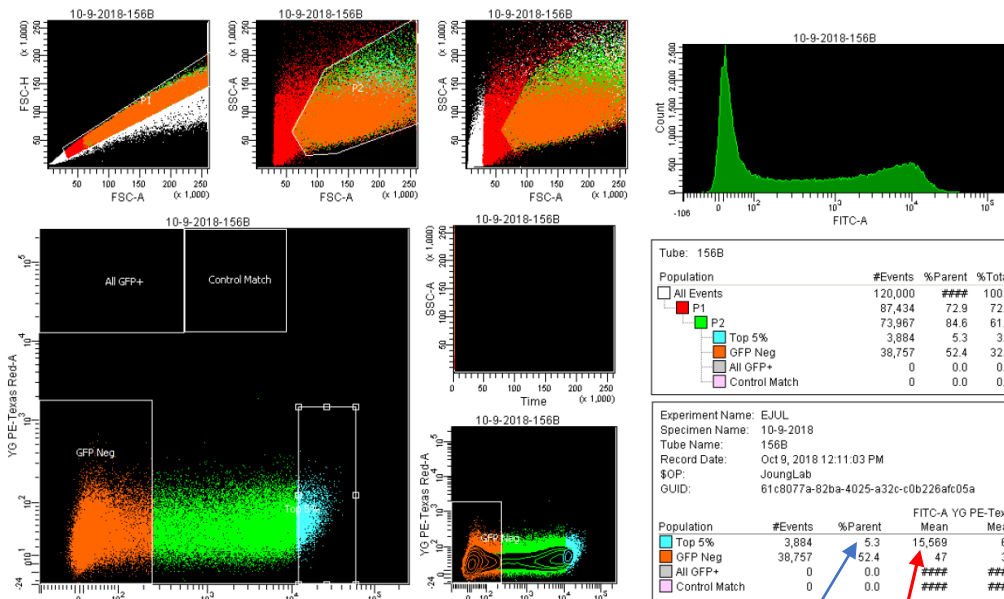
Top 5% signal population & GeoMean (MFI)

HEK293T Top 5%-matched NLS-nCas9-NLS Control for ABEmax



5% population with **GeoMean (MFI)**
matched to top 5% BE-treated cells (see next slide)

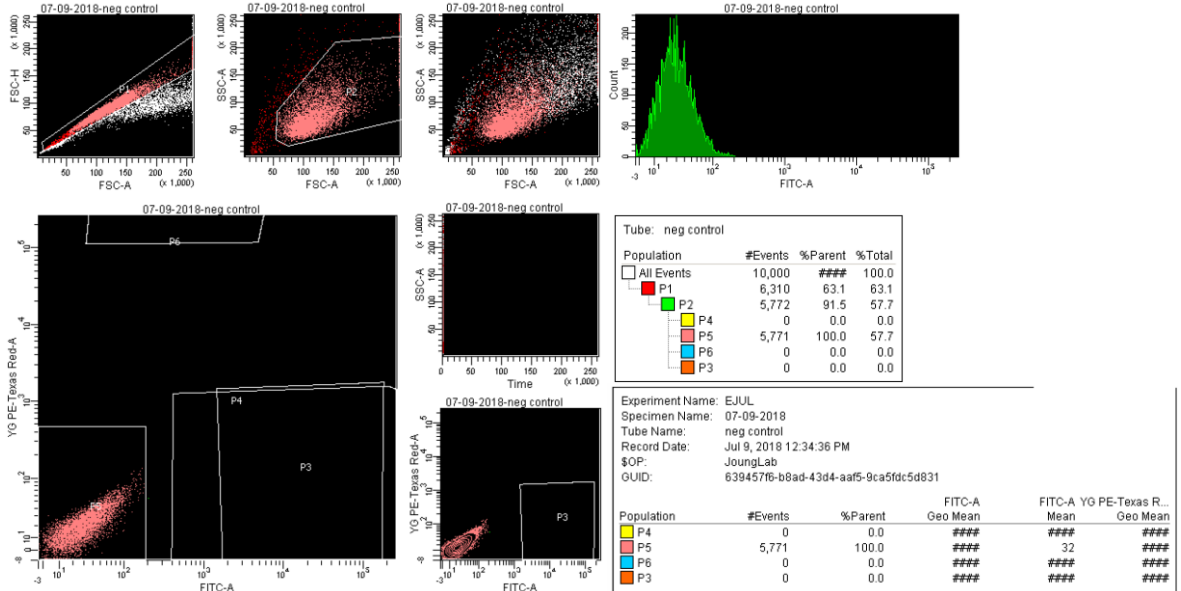
HEK293T Top 5% ABEmax-treated



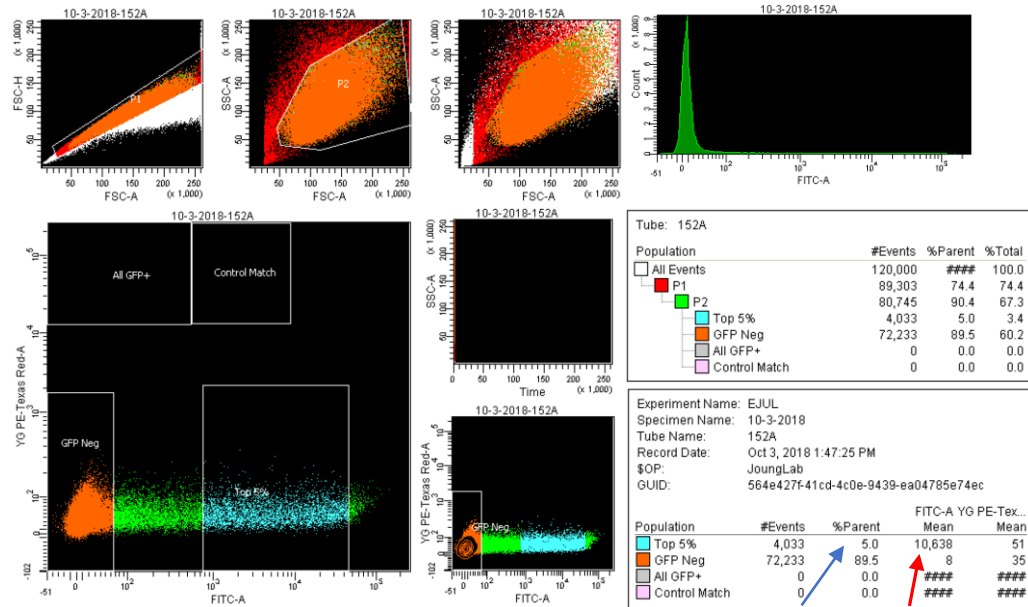
Top 5% signal population & **GeoMean (MFI)**

HepG2 cells

HepG2 Negative Control (no transfection)

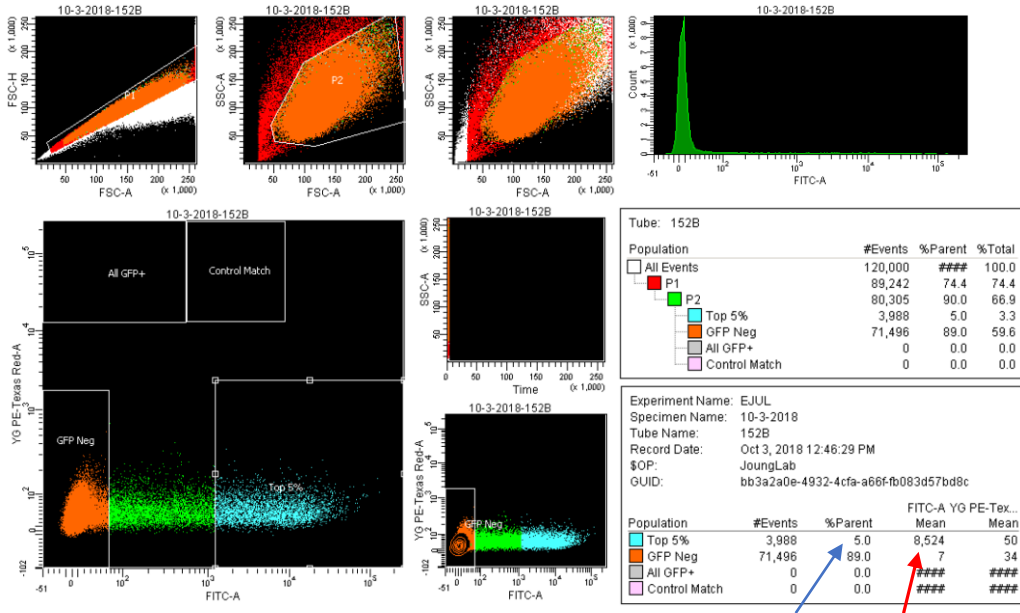


HepG2 Top 5%-matched nCas9-UGI-NLS Control for BE3



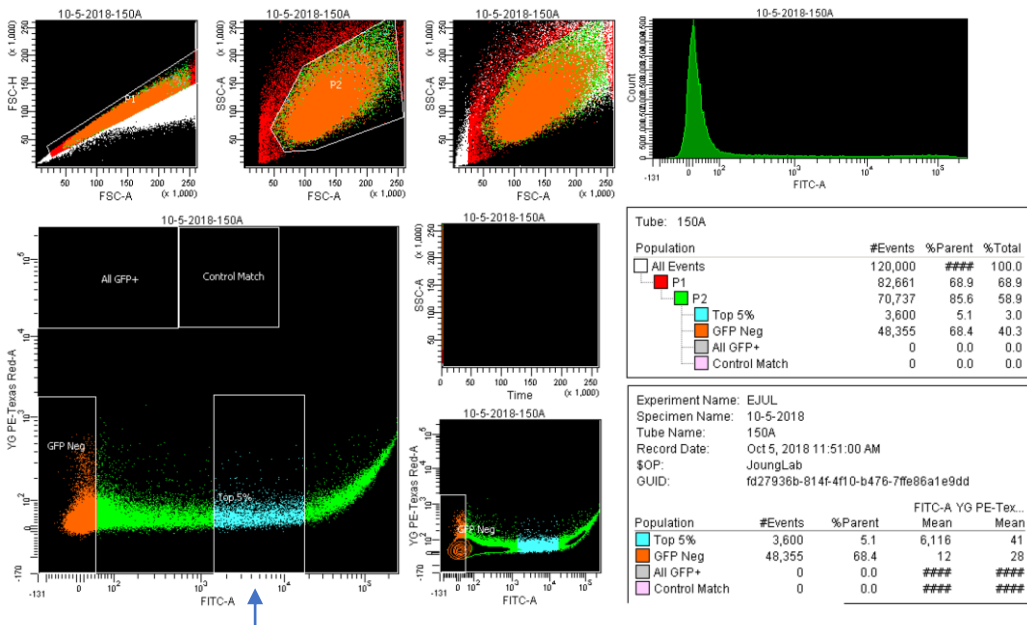
5% population with **GeoMean (MFI)** matched to top 5% BE-treated cells (see next slide)

HepG2 Top 5% BE3-treated



Top 5% signal population & GeoMean (MFI)

HepG2 Top 5%-matched (e)GFP-only Control



Population MFI-matched with top 5% signal population of BE-treated experiment on the same day